Complex Polyion−Surfactant Ion Salts in Equilibrium with Water: Changing Aggregate Shape and Size by Adding Oil

Juliana S. Bernardes,[†] Jens Norrman,[‡] Lennart Piculell,[‡] and Watson Loh*[,†]

Institute of Chemistry, Universidade Estadual de Campinas (UNICAMP), Caixa Postal 6154, 13083-970, Campinas, SP, Brazil, and Physical Chemistry 1, Center for Chemistry and Chemical Engineering, Lund University, P.O. Box 124, S-221 00 Lund, Sweden

Received: June 9, 2006; In Final Form: September 6, 2006

The phase behavior of ternary mixtures containing an alkyltrimethylammonium polyacrylate complex salt, water, and a nonpolar "oil" (*n*-decanol, *p*-xylene or cyclohexane) is investigated. The complex salts were prepared with short or long polyacrylates (30 or 6000 repeating units) and with hexadecyltrimethylammonium or dodecyltrimethylammonium surfactant ions. Phase diagrams and structures were determined by visual inspection and small-angle X-ray scattering analyses. Systems containing decanol display a predominance of lamellar phases, while hexagonal phases prevail in systems containing *p*-xylene or cyclohexane. The difference is interpreted as a result of the different locations of the oils within the surfactant aggregates. Decanol is incorporated at the aggregate interface, leading to a decrease in its curvature, which favors the appearance of lamellar structures. *p*-Xylene and cyclohexane, on the other hand, are mostly incorporated in the interior of the cylindrical aggregate, as reflected by its swelling as the oil content increases. The comparison of these results with those reported for similar systems with monovalent (bromide) counterions indicates a much more limited swelling of the lamellar phases with polymeric counterions by water. This limited swelling behavior is predominantly ascribed to bridging due to the polyions.

Introduction

Association between charged polymers and oppositely charged surfactants in aqueous solutions may lead to phase separation forming a concentrated phase rich in polyions and surfactant ions, and a more dilute phase, which mostly contains simple ions. The concentrated phases may display a variety of supramolecular structures with diverse and interesting properties, due to self-assembling tendency of surfactants, and hence they have been the subject of many recent investigations. These phases display structures that may be related to those formed by surfactants with monomeric counterions, but important contributions from the polymeric counterions are reported both in terms of facilitating the formation of the liquid crystalline structures as well as in modifying their features.[1,2] These liquid crystalline phases have found applications in the field of controlled drug delivery[3,4] and in templating the synthesis of materials with tailored geometries.[5,6]

A complete description of the phase equilibria in these systems is quite demanding, because addition of polyelectrolyte and oppositely charged surfactant to water leads to the formation of a four-component system, where any equilibrium phase can be described as a mixture of water and three of the four combinations of the four ions into neutral salts. This problem was addressed by Thalberg and co-workers,[7] who proposed that a convenient and comprehensive representation of such mixtures was in terms of a pyramidal (tetragonal) phase diagram. The apexes of the pyramid represent the five pure components: water, polyelectrolyte (polyion + simple ion), surfactant (surfactant ion + simple ion), complex salt (polyion + surfactant ion), and simple salt (simple cation + simple anion). A simplified approach to oppositely charged polymer−surfactant mixtures has recently been proposed by Piculell et al.,[1] involving the preparation of the pure complex salt as one species, allowing the investigation of true binary mixtures (complex salt + water) and ternary ones (complex salt + water + surfactant, or complex salt + water + polyelectrolyte).[1]

Using this approach, Svensson et al. investigated the phase behavior of binary mixtures of water and complex salts formed by cationic surfactants of different alkyl chain lengths ($n = 8$ to 16) with polyacrylate.[8] Ternary mixtures containing some of these complex salts and sodium polyacrylate or cationic surfactants with different counterions also had their phase diagrams determined,[2] as well as the structures of some of the liquid crystalline phases formed. These analyses gave an insight into the role of each component in the mesophase structure and stability. These studies revealed the key role of the attraction between polyions and surfactant aggregates in the formation of liquid crystalline structures, with important contributions from the polyions bridging between the aggregates,[1] while monovalent counterions favor the formation of homogeneous micellar phases that can be infinitely diluted with water.

An overall aim of systematic studies of associating polymer−surfactant mixtures, including oppositely charged mixtures, is to establish a thorough understanding of the factors that control the structures and the maximum water uptake of these mixtures. Such an understanding will make it possible to design systems with desired properties. Previous investigations of complex salts have indicated that the shape and size of the surfactant aggregate is one key factor in this context.[1] The present investigation focuses more strongly and systematically on this aspect, by using added nonpolar components, "oils", as a means to control the

* Corresponding author. E-mail: wloh@iqm.unicamp.br. Phone: + 55 19 3521 3148. Fax: + 55 19 3521 3023.
[†] UNICAMP.
[‡] Lund University.

10.1021/jp0636165 CCC: $33.50
Published on Web 10/28/2006

size and shape of the surfactant aggregates. Following the approach developed by one of our laboratories,[1] complex salts of two alkyltrimethylamonium surfactants ($C_{12}TA^+$ and $C_{16}TA^+$) with two polyacrylates of different degrees of polymerization (PA_{30} and PA_{6000}) were prepared. These complex salts will be referred to as $C_{12}TAPA_{30}$, $C_{16}TAPA_{30}$, $C_{12}TAPA_{6000}$, and $C_{16}TAPA_{6000}$, respectively. Their ternary mixtures with water and each of the three oils decanol, *p*-xylene, and cyclohexane were investigated with respect to their phase diagrams, and the phase structures were determined by small-angle X-ray scattering (SAXS) analyses. These particular oils were chosen due to their different polarities and the presumed differences in their locations within the surfactant aggregates. A more detailed analysis was performed for mixtures with decanol, and these results were compared to those reported by Fontell et al.[9] for the analogous ternary mixtures of water + decanol + $C_{16}TABr$ or $(C_{16}TA)_2SO_4$. The latter comparison allows a direct assessment of the effects of replacing bromide by divalent or polymeric counterions.

Experimental Section

Chemicals. Poly(acrylic acid), PAA, samples with molar masses of 2000 and 450 000 g mol^{-1} (30 and 6000 AA units, respectively), from Sigma, were used without further treatment. Some PAA samples were dialyzed according to a previous procedure,[1] but no differences were observed between complex salts when compared to nondialyzed PAA samples. Cationic surfactants dodecyltrimethylammonium and hexadecyltrimethylammonium bromides, ($C_{12}TABr$ and $C_{16}TABr$, respectively), with 99% purity, were purchased from Sigma. The oils used were decanol (from BDH p.a.), *p*-xylene and cyclohexane (both from Acros 99%), all of the highest purity available and used as received. Cationic ion-exchange resin, Dowex 550OH, from Sigma, was activated by washing with 1 mol L^{-1} NaOH under stirring for 1 h, followed by washing with Millipore water until neutral pH.

Synthesis of Complex Salts. The complex salts were prepared following the procedure developed by Svensson.[1] First the surfactants were converted into their OH forms by using an activated anionic ion-exchange resin. Typically, for 10 g of surfactant, 300 g of resin was used (in three stages). For each stage, 100 g of resin was mixed with surfactant and ca. 100 m L of water, under stirring for 1 h. This mixture was filtered and washed producing ca. 200 mL of C_nTAOH solution. The final solution, ca. 600 mL, was immediately refrigerated to avoid surfactant decomposition. Titrimetric analysis of the bromide content, following previous procedure,[1] confirmed that the ion exchange was complete.

The surfactant solution was titrated with an aliquot of a 3.5 wt % solution of poly(acrylic acid) with pH measurements using a standard glass electrode. The equivalence point was previously determined and occurred around pH 9. The poly(acrylic acid) solution was added dropwise to the remaining surfactant solution until a pH slightly above the equivalence point was reached. This mixture, containing the white concentrated top phase of complex salt, was left overnight in a refrigerator. The pH was then adjusted to the equivalence pH by adding more PAA and the complex salt was freeze-dried. The product, a white hygroscopic powder, was stored in a desiccator over silica gel, and the uptake of water under these conditions was determined to ca. 10 wt. % (this was taken into account in determining exact sample compositions). For the complex salts $C_{16}TAPA_{30}$ and $C_{16}TAPA_{6000}$, elemental analyses were performed, using a Perkin-Elmer Series II CHNS/O Analyzer 2400 equipment, providing carbon and nitrogen contents within 1% of agreement with a 1:1 (surfactant/AA monomer) complex salt stoichiometry.

Sample Preparation and Characterization. The desired amounts of complex salt, water, and oil were added to glass tubes, which were flame sealed (care was taken to avoid heating the samples) and mixed in a Vortex agitator. These samples were centrifuged upright and upside-down for a few days, and left at 25 °C to equilibrate for many weeks. Some samples were subjected to SAXS analyses after a few months to check for changes, and no significant differences were observed.

Samples were visually inspected for determination of the number of phases and their volumes. Samples were also examined between crossed polarizers for birefringence to identify presence of anisotropic (lamellar or hexagonal) phases.

Phase structures were determined by SAXS analyses. Two instruments were used for this purpose. Some SAXS spectra were recorded at Lund University using a Kratky compact small-angle system, with linear collimation and radiation at the wavelength of 1.54 Å, sample-to-detector distance of 277 mm, and a position-sensitive detector. Samples were housed in a cell with mica windows under temperature control. Typical acquisition times were longer than 1 h and the SAXS spectra were treated with the software 3D-view.

For other samples, the SAXS beamline (D11A) of the Brazilian Synchrotron Laboratory (LNLS), in Campinas, Brazil, was used. The experimental setup involved the use of X-rays at the wavelength of 1.608 Å and a sample-to-detector distance of 611.1 mm. For these experiments, a sample cell with mica windows was used, allowing temperature control (all measurements were made at 25 °C). The collected data were treated using the software TRAT1D, which allows for corrections for detector homogeneity, incident beam intensity, sample absorption, and blank subtraction (the empty cell was considered as a blank).[10] Typical acquisition times were ca. 15 min. No major differences were observed between spectra from these two sources, and, in both cases, longer acquisition times did not produce better resolution for other peaks in the SAXS spectra.

Results

In this section, the results will be presented in the following order. First, the approach adopted for the determination of the phase diagrams is described, followed by an outline describing general features of the different phase diagrams. In further sections, detailed analyses of each phase diagram along with structural analyses of the most relevant systems are presented. A complete description of all the investigated phase diagrams (all phase diagrams and tables containing compositions and structures determined for all of the samples studied) is available as Supporting Information.

Strategy of Investigating the Phase Diagrams. Ternary mixtures of each of the four complex salts ($C_{12}TAPA_{30}$, $C_{16}TAPA_{6000}$, $C_{12}TAPA_{6000}$, $C_{16}TAPA_{6000}$) with water and decanol were investigated. In addition, mixtures containing water, *p*-xylene, and $C_{16}TAPA_{6000}$, or water, cyclohexane, and the complex salts $C_{16}TAPA_{30}$ or $C_{16}TAPA_{6000}$, were investigated. The general approach for investigation of all phase diagrams was to focus on two main dilution lines, here called the water and oil dilution lines, respectively, as shown in Figure 1. Due to the almost complete immiscibility between water and the various oils used, the added water will enter only the aqueous microphase of the surfactant phases, whereas the added oil will mix only with the surfactant aggregates. In both cases, this approach allows one to observe all the possible mesophases formed, as well as the maximum level of dilution of each

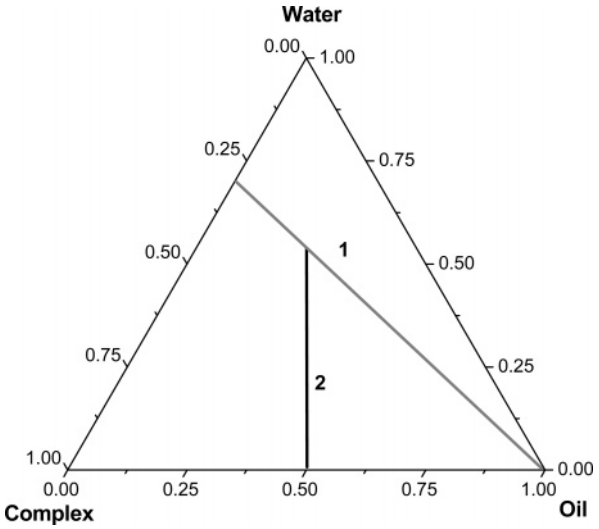

Figure 1. Schematic representation of the two dilution lines used in the present investigation: (1) oil dilution line; (2) water dilution line.

microphase. Water or oil added above this level will end up in separate phases of almost pure water or oil.

The oil dilution line starts from a binary mixture of complex salt and ca. 70% water, comprising a cubic or hexagonal phase in equilibrium with almost pure water (for a full description of the binary phase diagrams, see ref 1). Along this dilution line, the effects caused by the incorporation of oil into the surfactant aggregate can be followed. Excess water is present along most of the oil dilution line and, hence, the dilution is performed at a constant chemical potential of water. Three oils with different features were studied, in order of decreasing polarity: *n*-decanol, a typical cosurfactant, *p*-xylene, an aromatic solvent, and cyclohexane.

The water dilution line investigated in the phase diagrams represents the addition of water to a 50:50 (by weight) mixture of complex salt and oil. Samples with other compositions were prepared in order to elucidate specific features of each diagram and boundaries between phases. The number of samples prepared to determine each phase diagram varied with its complexity between approximately 20 and 50 samples. The fact that an almost complete ternary phase diagram could be determined with relatively few samples illustrates the power of the approach. All phase diagrams were determined at 25 °C and compositions are expressed as weight fractions.

As a general feature of all phase diagrams, the incorporation of oil favors the development of structures with reduced curvature. However, the details of the incorporation of oil into the surfactant aggregates differ for the different oils. Figure 2 shows the phase sequences for the different systems investigated along the oil dilution line. Liquid crystalline hexagonal and lamellar phases are observed when decanol is added, whereas only a hexagonal mesophase is present with *p*-xylene and cyclohexane. Moreover, different amounts of oil are needed to induce phase transitions and the appearance of a separated oil phase, which indicates saturation of the aggregate with respect to incorporation of oil. The solubility of the complex salts is different in the three oils: while decanol is capable of dissolving ca. 20% of the complex salts, their solubilities in *p*-xylene and cyclohexane are too small to be detected (smaller than 1%). Hence, the nature of the oil phase appearing at higher solvent contents differs, being reasonably approximated as pure oil for *p*-xylene and cyclohexane, but constituting a complex salt solution in decanol. The exact nature of the latter organic solution was not determined in this study, only that it was a visually isotropic low-viscous liquid.

Ternary Systems Containing *p*-Xylene and Cyclohexane. The liquid crystalline phases present in the investigated ternary systems containing *p*-xylene or cyclohexane are the hexagonal phase and, probably (see below), the lamellar phase. The normal hexagonal phase appears in equilibrium with both excess water and excess oil, and there is a three-phase triangle where all these phases coexist.

With *p*-xylene and $C_{16}TAPA_{6000}$, as shown in Figure 3, at low oil content the systems contained in region H+W represent

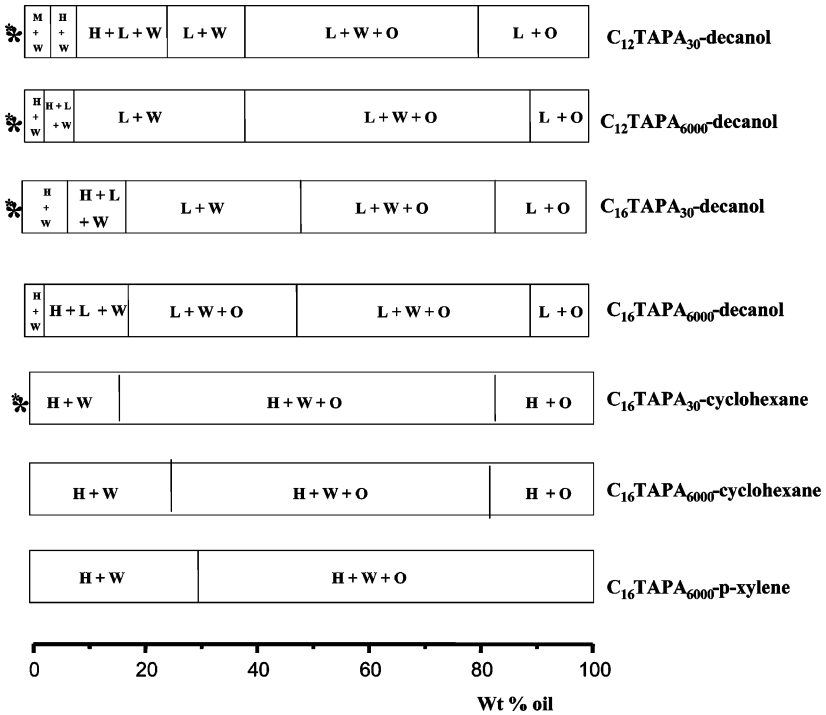

Figure 2. Phase evolution along the oil dilution line (as a function of the oil content), for the different systems investigated. Codes for phases: W, water; M, disordered micellar; H, hexagonal; L, lamellar; and O, oil. (*narrow cubic phase not shown here).

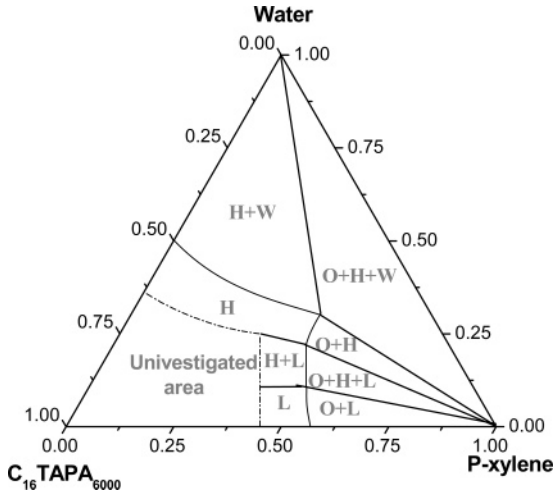

Figure 3. Phase diagram of the *p*-xylene/water/$C_{16}TAPA_{6000}$ system at 25 °C. Codes for phases: W, water; H, hexagonal; L, lamellar; and O, oil.

biphasic systems containing a hexagonal phase in equilibrium with excess water. As more *p*-xylene is added to the mixture, it is incorporated into the surfactant aggregates that comprise the hexagonal phase. This leads to a continuous increase in the cell parameter from 46 to 78 Å when the *p*-xylene content increases from 0 to ca. 25 wt. %, as revealed by the SAXS spectra shown in Figure 4. Along this line, the maximum amount of *p*-xylene that can be incorporated into the hexagonal phase corresponds to an oil/surfactant mass ratio of 7:3. Addition of more oil leads to the appearance of an excess oil top phase, with the formation of a three-phase system (represented by region O+H+W in Figure 3).

Specifically along this dilution line, addition of more *p*-xylene will only increase the volume of the oil phase, which may be approximated as pure *p*-xylene due to the negligible complex salt solubility.

Experiments along the water dilution line revealed, at low water contents (region L in Figure 3), a liquid crystalline phase with a first reflection peak at $q = 0.132$ Å^{-1}, see Figure 5. We tentatively identify this structure as a lamellar phase, as will be justified in more detail shortly. At higher water contents, a two-phase lamellar-hexagonal area (region H+L) was revealed by SAXS spectra (not shown) that could be identified as superpositions of spectra from regions L and H. In principle, the limited resolution of the spectra from the lamellar phase does not allow us to entirely exclude the possibility of an inverted hexagonal structure for region L. However, this possibility was ruled out for two reasons. First, this would imply a coexistence of a normal and an inverted hexagonal structure in region H+L, and such coexistence has, to our knowledge, never been observed; between a normal and an inverted hexagonal phase there is generally a lamellar phase. Second, our results for the mixtures with decanol (see below) did not show any inverted hexagonal phase, despite the fact that decanol is much more effective than *p*-xylene in reducing the curvature of the surfactant aggregate.

Selected samples off of the water dilution line were entirely consistent with the above phase diagram. Region O+L displays two phases in equilibrium: a lamellar liquid crystalline phase in equilibrium with a top oil phase, while region O+H+L is a three-phase region containing the lamellar phase, the hexagonal phase, and excess oil. Region O+H in this phase diagram represents a biphasic region where a normal hexagonal phase is in equilibrium with a top oil phase.

All boundaries indicated in Figure 3 were quantitatively determined either by investigating samples close to the boundaries, or by estimates based on the lever rule. Using the boundary between regions H+W and H (Figure 3) as an example, samples located within region H were inspected to determine their volume ratios and, assuming the density of both phases to be equal to 1 g cm^{-3}, their respective mass fractions were calculated allowing, by use of the lever rule, determination of the distance between the global composition point and the phase boundary. Tie-lines were assumed to pass through the apex of the triangle, due to the almost complete immiscibility of oil with water and complex salts.

Phase diagrams of the two complex salts mixed with cyclohexane, not shown here (but available as Supporting Information), display essentially the same features, including the regions L and H+L at low water contents. The exact positions of the phase boundaries vary somewhat with the complex salt and the oil, as indicated in the diagram of Figure 2. These hexagonal phases display cell parameters that increase, respectively, up to 71 or 89 Å within this biphasic region, again larger than the value reported for the equivalent binary mixture (ca. 46 Å)[2], with the larger distances corresponding to the complex salt with the polymer of higher molar mass. For the

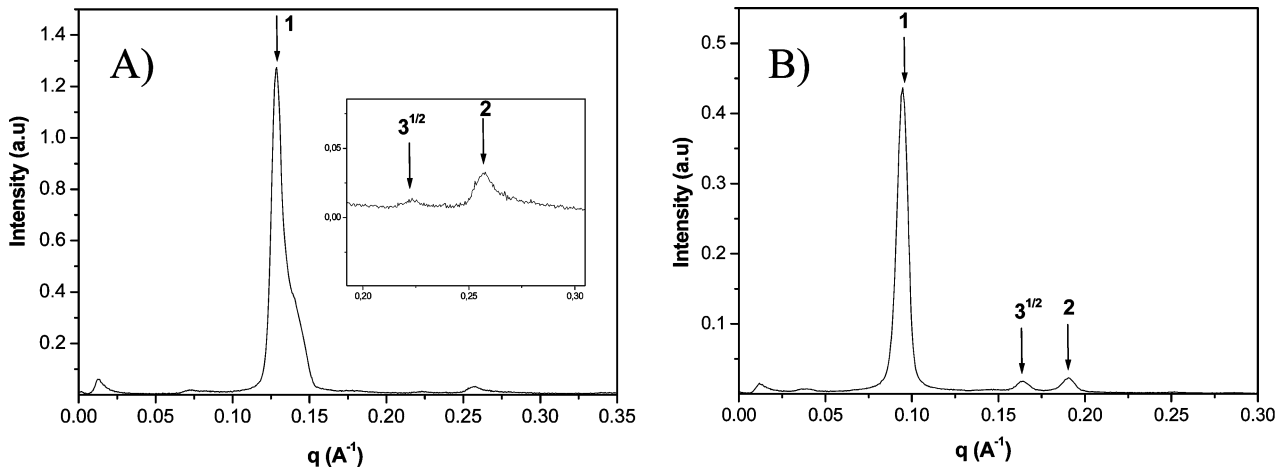

Figure 4. SAXS spectra of hexagonal phases in the H+W two-phase region of the system *p*-xylene/water/$C_{16}TAPA_{6000}$, with the relative peak positions indicated. (A) lattice parameter = 56 Å (composition: 7 wt. % of *p*-xylene, 71 wt. % of water, and 22 wt. % of $C_{16}TAPA_{6000}$); (B) lattice parameter = 78 Å (composition: 26 wt. % of *p*-xylene, 56 wt. % of water, and 18 wt. % of $C_{16}TAPA_{6000}$).

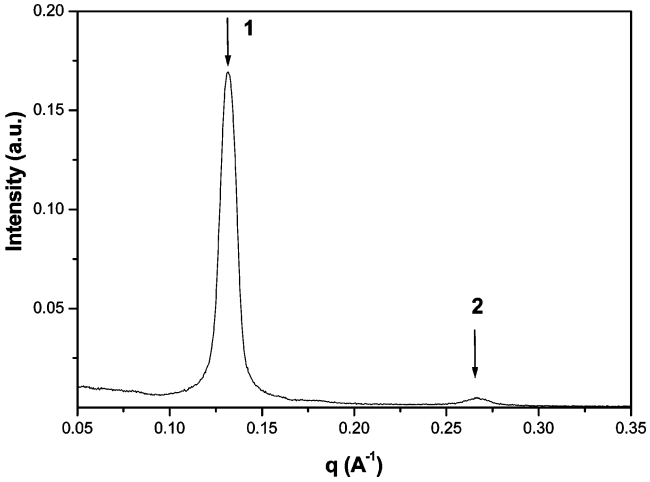

Figure 5. SAXS spectrum of a sample contained in region L (composition: 49 wt. % of *p*-xylene, 5 wt. % of water, and 46 wt. % of $C_{16}TAPA_{6000}$).

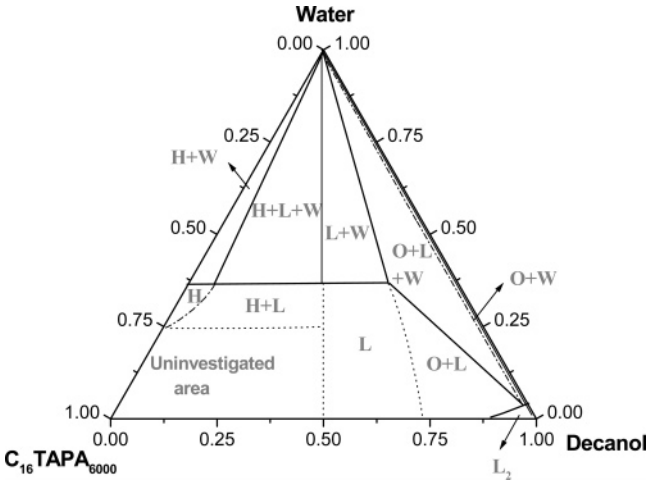

Figure 6. Phase diagram of the decanol/water/$C_{16}TAPA_{6000}$ system at 25 °C. Codes for phases: W, water; H, hexagonal; L, lamellar; O, oil, L_2-isotropic decanolic solution. Borderlines were quantitatively determined as detailed in the text, except for the dotted lines, which represent estimates.

$C_{16}TAPA_{6000}$ complex salt, the cell parameter values observed with cyclohexane were consistently larger than those with *p*-xylene.

Within the three-phase regions of these phase diagrams, the phase structures determined by SAXS analyses remain essentially constant, as required by the Gibbs phase rule for an isothermal ternary three-phase system. These findings (which were also confirmed for systems containing decanol) confirm that these complex salt mixtures behave like truly ternary ones.

Ternary Systems Containing Decanol. All phase diagrams observed with ternary mixtures containing the four complex salts, water, and decanol were similar and may be represented by the one for $C_{16}TAPA_{6000}$, shown in Figure 6. In this case, two liquid crystalline phases are observed for the investigated ternary mixtures, the normal hexagonal, and a lamellar phase, with the latter dominating the phase diagram.

Considering the decanol dilution line, the dominating effect of this oil is to reduce the aggregate curvature. For systems with $C_{12}TAPA_{30}$, $C_{12}TAPA_{6000}$, and $C_{16}TAPA_{30}$, the starting binary mixture represents a biphasic system containing a cubic phase and excess water.[1] Addition of a minimum amount of decanol (less than 2 wt. %) leads to changes of the aggregate structure to generate a hexagonal phase. This amount of oil represents a molar ratio decanol/surfactant of less than 1:30, indicating a strong effect of this co-surfactant upon the aggregate curvature. Cubic phases containing decanol were observed only with the complex salt $C_{12}TAPA_{30}$ at up to 4% decanol.

TABLE 1: Characteristic Parameters of Lamellar Phases Formed by C_nTAPA_m Complex Salts in Ternary Systems with Water and Decanol, in the Biphasic Region (lamellar + excess water) of Their Phase Diagrams[a]

complex	composition range (wt % decanol)	d/Å	d_{hc}/Å	a_s/Å^2	lamella saturation
$C_{12}TAPA_{30}$	13−33	38−41	17−23	71−117	3:1
$C_{12}TAPA_{6000}$	18−48	38−42	20−27	78−172	6:1
$C_{16}TAPA_{30}$	13−39	42−48	21−29	77−140	5:1
$C_{16}TAPA_{6000}$[b]	44	48	30	168	6:1

[a] Repeating distance, d, bilayer thickness, d_{hc} and area per surfactant headgroup, a_s. The last column lists the maximum capacity of these lamellar phases for incorporation of decanol (expressed as molar ratio decanol: surfactant). [b] Only one data point was investigated for this system.

Mixtures containing the complex salt $C_{12}TAPA_{30}$, water, and 2−3% decanol appeared as biphasic with a top viscous phase and a bottom excess water phase. Depending on the manipulation of samples prior to SAXS analyses, the SAXS spectra obtained for the top phase (not shown) displayed features of either micellar (a broad peak) or liquid crystalline (cubic) phases. This observation agrees with a previous report[8] that, for complex salts with short-chain cationic surfactants (typically $n = 10$ or 12), the concentrated phases from different samples in the same two-phase region could be either disordered micellar or cubic. This feature was interpreted as reflecting closely similar Gibbs free energies of the disordered micellar and micellar cubic phases. Hence, small perturbations, possibly due to the polydispersity of the polyion, would shift the system between these two structures.

A comparative analysis of the phase evolution is visualized in Figure 2. As already pointed out, decanol addition favors reduction of the aggregate curvature, a general feature ascribed to its co-surfactant behavior and related to its intercalation between surfactant molecules at the aggregate interface. More precisely, it is the headgroup of the alcohol that is located at the interface. Further addition of decanol leads to an increase in the cell parameter of the hexagonal phase as the oil is incorporated into the surfactant aggregates, varying from ca. 43 to 46 Å and from 46 to 52 Å, respectively, for complex salts with C_{12} and C_{16}. These values are close to the value of 46 Å reported for mixture of the complex salt $C_{16}TAPA_{30}$ + water.[2] A more detailed analysis of characteristic parameters of hexagonal phases formed in the presence of the three oils will be presented in the discussion section.

Further addition of decanol leads to a phase transition with the appearance of a lamellar phase, which coexists with the hexagonal phase in a three-phase system (the third phase is excess water) at higher decanol contents. The decanol/surfactant mass ratios for the maximum uptake of decanol in the hexagonal phases with the four complex salts are: 1:4.7 with $C_{12}TAPA_{30}$; 1:3.5 with $C_{12}TAPA_{6000}$; 1:7 with $C_{16}TAPA_{30}$; and 1:8.7 with $C_{16}TAPA_{6000}$. These ratios are much lower than those observed with *p*-xylene and cyclohexane, in agreement with a higher capacity of decanol to reduce the aggregate curvature.

Additionally, the amount of decanol needed to induce formation of the lamellar phase is smaller for C_{16} than C_{12} complex salts, as can be also seen in Figure 2, in agreement with the expected trend considering geometric considerations as the critical packing parameter.[11] Lamellar phases are also obtained with smaller decanol contents for complex salts with

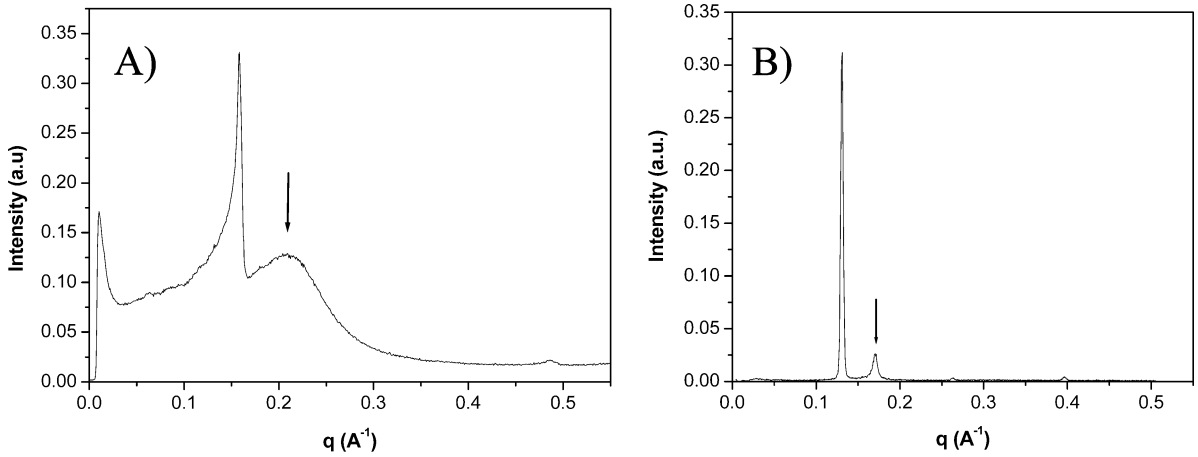

Figure 7. SAXS spectra for samples of: (A) $C_{12}TAPA_{30}$ + decanol + water (composition: 28 wt. % of decanol, 46 wt. % of water, and 26 wt. % of $C_{12}TAPA_{30}$); (B) $C_{16}TAPA_{6000}$ + decanol + water (composition: 36 wt. % of decanol, 45 wt. % of water, and 19 wt. % of $C_{12}TAPA_{6000}$). Broad peaks indicated by arrows.

PA_{6000}, suggesting that this larger polyanion also favors a reduced curvature of the aggregate.

The characteristic parameters for the lamellar phases formed by the four complex salts mixed with decanol in the biphasic region (lamellar + water) are expressed in Table 1, including repeat distances,

$$d = \frac{2\pi}{q} \tag{1}$$

bilayer thicknesses,

$$d_{hc} = d\phi_{hc} \tag{2}$$

and the areas per surfactant headgroup,

$$a_s = \frac{2(n_s v_s + n_o v_o)}{n_s d_{hc}} \tag{3}$$

Details on how these parameters were estimated are given in the Supporting Information accompanying this paper.

As expected, thicker bilayers are observed for the C_{16} complex salts in comparison with those formed by C_{12} complex salts. However, in both cases the thickness of the bilayers is smaller than twice the length of these alkyl chains, 2 × 17 Å for C_{12} and 2 × 22 Å for C_{16}.[11] Likewise, the difference in thickness for C_{16} and C_{12} bilayers is less than that estimated from these chain lengths, as commonly found for surfactant bilayers.[11]

It is clear from Table 1 that, as expected, a_s values increase with the addition of decanol. The values for d and d_{hc} also increase, but not so pronouncedly, upon decanol addition. The facts that the repeat distance and the bilayer thickness change little with the addition of decanol, while the area per surfactant headgroup increases quite substantially, indicate that this oil acts as a co-surfactant with the headgroups located at the aggregate interface. Moreover, it is interesting that the repeat distances are not affected so much by the added co-surfactant, despite the fact that the area per surfactant headgroup grows significantly in the studied interval. In all cases, the polyion effectively pulls the lamella together.

For some SAXS spectra of lamellar samples a broad peak was observed at 0.18−0.22 Å^{-1}, as shown in Figure 7. This peak does not belong to reflection peaks due to liquid crystalline structures—it is much broader and its position does not match the expected sequence for these phases. Similar peaks have been observed previously in lamellar surfactant phases with and without incorporated polymer molecules[12−14] and have then been shown to emanate from pseudoperiodic or periodic correlations in the lamellar plane. In systems without incorporated polymer, the correlations have been attributed to deformations of the lamellar structure. In lamellar lipid phases containing DNA,[12] the peaks could be explained as correlation distances between DNA chains. In the system investigated in this work, it seems likely that the correlations are caused by the polyacrylate molecules in the lamellar plane both directly and indirectly, since the presence of the polyion will induce a nonhomogeneous distribution of surfactant and co-surfactant molecules in the lamellar plane.

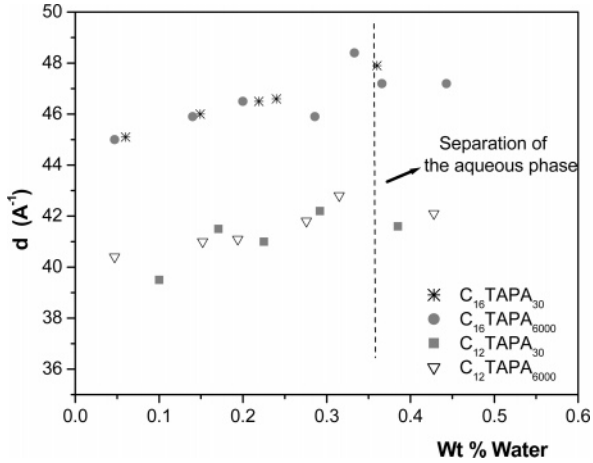

Figure 8. Swelling of the lamellar phases formed with the different complex salts at a 50:50 decanol/complex salt mass ratio, as a function of the water content. The dotted line indicates the appearance of a separated water phase.

The lamellar phase is capable of incorporating decanol up to a saturation point, after which a top decanol phase appears, as represented by a three-phase triangle in the phase diagram. The molar ratios for saturation of the lamellar phases, listed in Table 1, suggest higher decanol incorporation into the phases formed with the larger PA. The saturation values listed in Table 1 refer to the limits of the two-phase region (lamellar + excess water).

The effect of a polymeric counterion on the swelling of the lamellar phases by diluting with water (represented by dilution line 2 in Figure 1) was also investigated. These results are summarized in Figure 8, which shows that the lamellar phases of all complex salts containing equal amounts (by weight) of decanol and surfactant swell upon addition of water up to a

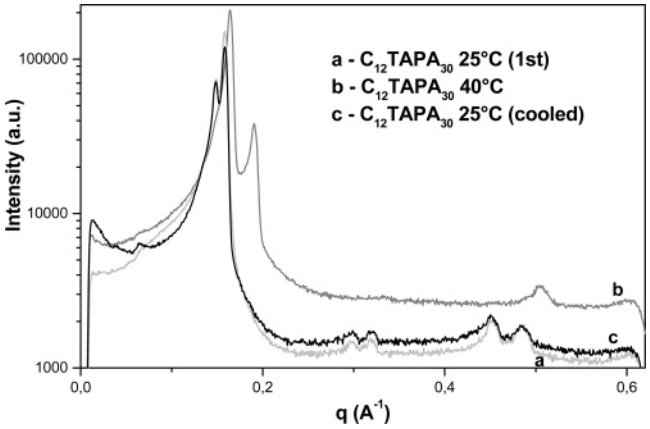

Figure 9. SAXS spectra of a sample containing $C_{12}TAPA_{30}$ + decanol + water (composition: 23 wt. % of decanol, 37 wt. % of water, and 40 wt. % of $C_{12}TAPA_{30}$) displaying two lamellar phases, performed at 25 °C and 40 °C (see text for details).

saturation limit, ca. 35 wt %, after which excess water added forms a second phase.

A striking observation was made investigating lamellar phases at high water content (close to saturation by water). In that region, SAXS spectra were recorded with evidence of two lamellar phases, as shown in Figure 9. The region of coexistence for these lamellae includes mixtures that were macroscopically homogeneous as well as some with the presence of a separate excess water phase. Similar SAXS spectra were obtained for mixtures of all of the four complex salts with water and decanol, and all occurred in similar locations of the phase diagrams. A coexistence of two lamellar surfactant phases has previously been addressed both from a theoretical[15] and from an experimental point of view. The experimental evidence refers to a diversity of systems formed by polymeric surfactants,[16] mixtures of surfactants,[17] polymers and lipids,[18] and polycations and SDS.[19] In the present investigation, a mixture with $C_{12}TAPA_{30}$ containing two coexisting lamellar structures was investigated in more detail in order to discriminate whether this situation represented an equilibrium state. SAXS spectra were recorded in the mixture prepared and equilibrated as mentioned in the Experimental section (see Figure 9). Later, this same mixture was heated to 40 °C for a few hours and its SAXS spectrum revealed that the phases most probably remained lamellar but now displaying shorter repeating distances (peaks shifted to larger q values). After that, the system was re-equilibrated at 25 °C, and its SAXS spectrum showed the same peaks as before heating. This thermoreversibility is a necessary, although not sufficient, criterion for equilibrium state. Interestingly, results from ongoing investigations on related systems comprising complex salts of $C_{16}TA^+$ with polyacrylate and polymethacrylate mixed with octanol also show evidences for coexistence of two lamellar phases in similar positions of the phase diagram.[20]

Discussion

Structural Analyses of Hexagonal Phases with Respect to the Location of the Oils in the Aggregate. For the systems prepared with *p*-xylene and cyclohexane, the normal hexagonal phase was the dominating liquid crystalline phase, as shown in Figure 3. Systems containg decanol, on the other hand, displayed a predominance of lamellar phases, with only a limited region where hexagonal phases were observed, as can be seen in Figure 6.

To investigate further the reasons why different structures dominate depending on the oil used, we have refined the analysis of the structural information provided by SAXS, aiming at determining the preferred location of these oils within the surfactant aggregates.

The incorporation of oil into a surfactant aggregate can be analyzed according to two limiting situations: (i) penetration, where the oil acts as a cosurfactant with its headgroups positioned between neighbor surfactant molecules at the aggregate interface, which should lead to an increase in the effective area per surfactant headgroup; and (ii) swelling, with the cosolvent located in the core of the aggregate, which should lead to an increase in the aggregate radius or thickness.

One way of discriminating between these two limit cases was put forward by Kunieda and co-workers[21,22] through analyses of changes in the area per surfactant headgroup and the aggregate dimensions as functions of the oil content.

For a hexagonal phase, the radius of the hydrocarbon core of a cylindrical aggregate, r_{hc}, can be estimated as[23]

$$r_{hc} = \sqrt{\frac{\phi_{hc} 2d^2}{\sqrt{3}\pi}} \tag{4}$$

where d is the distance between adjacent planes of the hexagonal structure, which can be obtained from the position of the first peak in the SAXS spectrum and ϕ_{hc} is the volume fraction of the hydrocarbon portion of the aggregate, that is, the surfactant chains plus the dissolved oil. In a first approximation, ϕ_{hc} may be taken as the sum weight fraction of surfactant hydrocarbon chains and oil, assuming that both oil and surfactant are fully incorporated into the aggregates and that the hydrocarbon density is equal to 1 g cm^{-3}. This approach further assumes that the surfactant headgroups are located into the aqueous microphase; hence, this radius of the cylindrical aggregate refers only to its hydrocarbon core.

The average area per surfactant headgroup at the surface of the hydrocarbon core, a_s, may be obtained as[23]

$$a_s = \frac{2}{r_{hc}}\left(v_c + \frac{n_o}{n_s} v_o\right) \tag{5}$$

where r_{hc} is determined as above, n_o and n_s represent the numbers of moles of oil and surfactant, respectively, and v_c and v_o represent the volumes occupied by a surfactant hydrocarbon chain and an oil molecule, respectively.

Using the above relations, derived in the Supporting Information, the evolution of both parameters was analyzed within the biphasic region of the phase diagrams containing the normal hexagonal phase and excess water. The values shown in Figure 10 were obtained for the system $C_{16}TAPA_{6000}$ as a function of the *p*-xylene content. This approach led to consistent results for different mixtures in the same phase diagram.

Figure 10 shows two distinct regimes: At low *p*-xylene contents, the area per surfactant headgroup remains constant (ca. 65 $Å^2$), while the cylinder radius increases from less than 20 Å to ca. 30 Å. Above 58 vol %, the cylinder radius keeps increasing at an approximately unchanged rate, whereas the area per surfactant headgroup displays a steep increase reaching values of ca. 90 $Å^2$. The first regime is consistent with an incorporation of *p*-xylene only in the core of the surfactant aggregate, while at contents higher than 58 vol %, it seems that a fraction of the *p*-xylene molecules reside at the surface of the aggregate, causing an increase in the area ascribed to each surfactant headgroup. These results point to a preferential

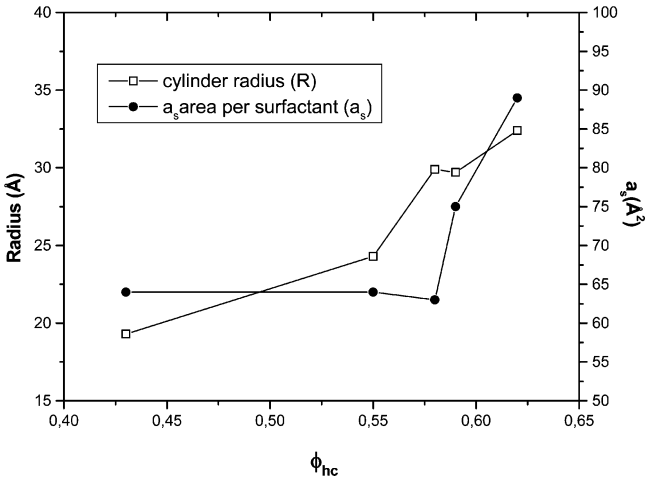

Figure 10. Evolution of the cylinder radius and area per surfactant headgroup, a_s, for hexagonal phases formed by $C_{16}TAPA_{6000}$ as a function of *p*-xylene content.

TABLE 2: Dimensions (radii) of Cylindrical $C_{16}TA$ Aggregates with Different Counterions

system	r_{hc}/Å	Ref
length of an extended C_{16} chain	21.8	(11)
binary system $C_{16}TABr$ + water (47% $C_{16}TABr$)	19.6	(24)
binary system $C_{16}TAPA_{30}$ + water (60% $C_{16}TAPA$)	16.0	(1)
ternary system $C_{16}TAPA_{6000}$ + water + *p*-xylene (46−26% of $C_{16}TAPA$ and 13−44% *p*-xylene)	19.3−32.4	this work

location of *p*-xylene molecules inside the aggregate, so that *p*-xylene enters the surface of the aggregate only at higher contents.

The same analysis is not possible for the hexagonal phases formed in the presence of decanol, since the hexagonal aggregates become lamellar at less than 1:3 decanol/surfactant molecules (ca. 4 wt. % along the working dilution line). This efficiency in switching the preferred geometry from hexagonal to lamellar is consistent, by itself, with decanol being located at the aggregate interface, as expected for co-surfactants such as long chain alcohols.

Dimensions (radii) of the cylindrical aggregates formed by $C_{16}TA^+$ surfactants with different counterions are listed in Table 2, for comparison. In all cases, these radii are smaller than the length of an extended C_{16} chain, as usual for nonspherical surfactant aggregates. By exchanging the surfactant counterion from bromide to PA, in a binary system with similar concentration, the radii decrease by ca. 20%. The radius with PA counterions increases again when *p*-xylene is added, eventually to values much larger than that of an extended C_{16} chain. As discussed before, addition of *p*-xylene may lead to radii larger than 30 Å, almost twice the value for the corresponding binary system.

Polyvalent Versus Mono- or Divalent Counterions. This section focuses on the analysis of possible structural differences arising from the presence of polymeric counterions, as opposed to mono and divavalent anions. For this, results obtained in the present investigation for the system $C_{16}TAPA_{30}$ + water + decanol are compared to those previously reported by Fontell and co-workers[9] for the systems $C_{16}TABr$ or $(C_{16}TA)_2SO_4$ + water + decanol.

Figure 11 allows the comparison of phase behavior in systems containing water, decanol, and CTA^+ with different counterions

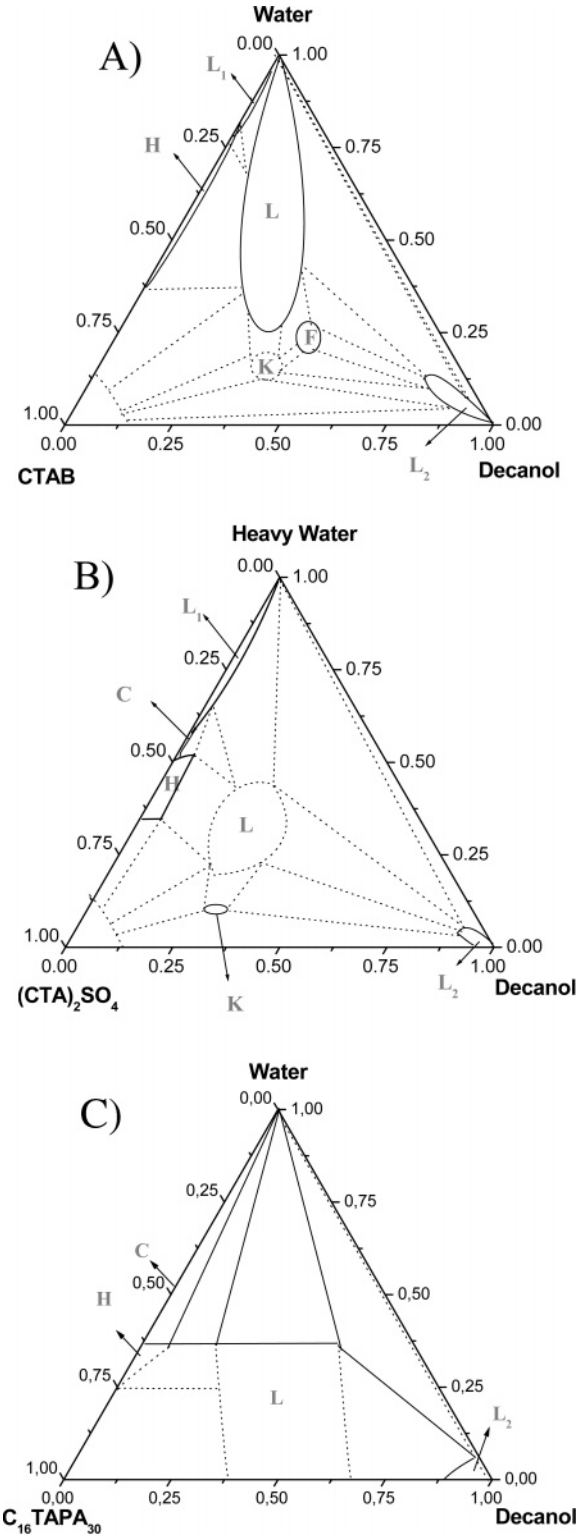

Figure 11. Comparison of phase diagrams for ternary systems containing water, decanol and: (A) $C_{16}TABr$,[9] (B) $(C_{16}TA)_2SO_4$,[9] or (C) $C_{16}TAPA_{30}$. The phases indicated in the diagrams are: L_1 and L_2-isotropic solution, C, cubic; H, hexagonal; L, lamellar; F, inverted hexagonal phase; K, non-hexagonal inverted rod-structure.

(bromide, sulfate, and polyacrylate). It is clear that, along the dilution line 1 represented in Figure 1, the phase sequences are similar. The curvature displayed by these liquid crystalline phases decreases as the decanol content increases, from a micellar (cubic micellar for $C_{16}TAPA_{30}$) to a normal hexagonal and then a lamellar phase, with prevalence of this last one. For

the three systems represented in Figure 11, only very small regions of micellar and hexagonal phases were observed, which demonstrates the efficiency of decanol in inducing the formation of lamellar phases.[9] At higher decanol contents a decanol-rich phase appears.

One difference observed when comparing the phase diagrams of C_{16}TAPA with those of C_{16}TABr in mixtures with decanol is that no inverted liquid crystalline phase was found with the polymeric anions, as opposed to the systems with bromide and sulfate counterions.[9] With C_{16}TABr + water + decanol, two inverted phases were found, an inverted hexagonal and another phase with an inverted rod structure, though nonhexagonal. With $(C_{16}TA)_2SO_4$, only this last inverted nonhexagonal phase was identified. An inverted hexagonal phase was also detected when stoichiometric complex salts formed by C_{16}TADNA were mixed with decanol and water.[25] The fact that no inverted phase was observed in the present studies with C_{16}TAPA complex salts may be related to a difficulty to packing the flexible polymeric counterion inside the aqueous compartment of these inverted phases. A different situation is at hand for DNA, which is a rigid rod that may align itself inside the aqueous channels of an inverted hexagonal phase, and which also carries a higher linear charge density than polyacrylate.

From the above, we may conclude that the aggregate geometry in the mixtures in Figure 11 is mainly determined by the content of co-surfactant, and only to a lesser degree by the nature of the counterion. By contrast, the ability of the various structures to absorb water is controlled by the nature of the counterion, and here, an interesting sequence can be observed.

With monovalent bromide counterions, both the infinite planar surfactant aggregates in the lamellar phase and the finite aggregates in the micellar phase repel each other, and both phases can absorb an almost unlimited amount of water. The high swelling is a result of the long-range repulsive force due to the entropy of mixing of the counterions, as correctly predicted by the mean field Poisson−Boltzmann theory.

With divalent sulfate counterions, the lamellar phase no longer swells. The attractive force in this case, which is not predicted by Poisson−Boltzmann theory, is due to ion−ion correlations, as was first shown in Monte Carlo simulations by Guldbrand et al.[26] Recently, Monte Carlo simulations have been used successfully to simulate phase equilibria in ternary lamellar surfactant systems with mono- and divalent counterions.[27] Interestingly, however, the small micellar aggregates are completely miscible with water, even with divalent counterions. The $(C_{16}TA)_2SO_4$ micelles, with no added decanol, make up a continuous micellar solution at high dilution. At lower water content, the micelles first pack into a micellar cubic phase, before a hexagonal phase forms, due to packing constraints, at still dryer systems. Again, this result is in agreement with recent Monte Carlo simulations,[28] where Linse and Lobaskin showed that the attraction due to divalent counterions is not sufficient to induce a phase separation of micelle-like charged spherical particles in water; counterions with a valency of three or higher are required.

In the $C_{16}TAPA_{30}$ system, finally, the counterions are flexible polyions, that give rise to a very strong attraction. This is sufficient to condense the spherical micelles into a cubic phase even in the presence of excess water. In this case, the attraction is due not only to ion correlation effects; simulations indicate that it is actually dominated by polyion bridging.[2]

Another difference when comparing lamellar structures with small and polymeric anions concerns the values of the area per surfactant headgroup. Larger values are obtained when the counterion is the longer PA (as listed in Table 1) in comparison with those reported for mixtures of C_{16}TABr + water + decanol of similar compositions (ca. 50−80 Å^2),[9] also confirming an important contribution of the polymeric counterion. Bilayer thicknesses, on the other hand, remain around 30 for both types of counterions.

Conclusion

The present systematic investigation gave detailed insights on how different oils are incorporated into assemblies of complex surfactant salts with polymeric counterions, and their consequent effect in terms of structural changes. Oils that are more apolar, such as *p*-xylene and cyclohexane, tend to be incorporated in the core of the surfactant aggregates, favoring the formation of hexagonally packed cylinders, which swell as the oil content is increased. Systems containing decanol, however, are dominated by lamellar phases, which can be ascribed to the incorporation of decanol at the aggregate interface, favoring the decrease in the aggregate curvature.

Comparisons with previous phase studies of cationic surfactants with mono- or divalent counterions, mixed with decanol, show that similar structural changes are induced by added decanol, regardless of the nature (mono- di- or polyvalent) of the counterions—except that no inverted phases are found, at least not with polyacrylate as the counterion. By contrast, strong effect of changing the counterion is found in the ability of the various structures to absorb water. Both micellar and lamellar systems swell indefinitely in water when the counterions are monovalent. With divalent counterions, only the micellar system swells; the lamellar system shows limited swelling owing to attractive ion−ion correlation effects. In systems with polymeric counterions the attraction, caused mainly by polyion bridging, is sufficiently strong to pull the micelles into a concentrated cubic phase, which does not swell in the presence of excess water.

Acknowledgment. The authors gratefully acknowledge the Brazilian Agency FAPESP for financial support to this work in the form of a PhD scholarship to J.S.B. and of travel grants to W.L. and L.P., which allowed visits between Lund and Campinas. J.N. thanks Per Westlings memorial fund for travel grants for a visit to Campinas. W.L. also thanks the Brazilian Agency CNPq for a senior researcher grant. The Brazilian Synchrotron Laboratory, LNLS, is also acknowledged for the use of the SAXS beamline and the support of the line staff. L.P. thanks the Swedish Research Council (VR) for a research grant.

Supporting Information Available: Complete description of all the investigated phase diagrams (all phase diagrams and tables containing compositions and structures determined for all of the samples studied). This material is available free of charge via the Internet at http://pubs.acs.org.

References and Notes

(1) Svensson, A.; Piculell, L.; Cabane, B.; Ilekti, P. *J. Phys. Chem. B* **2002**, *106*, 1013.

(2) Svensson, A.; Piculell, L.; Karlsson, L.; Cabane, B.; Jönsson, B. *J. Phys. Chem. B* **2003**, *107*, 8119.

(3) Bronich, T. K.; Nehls, A.; Eisenberg, A.; Kabanov, V. A. *Colloids Surf. B* **1999**, *16*, 243.

(4) Kabanov, A. V.; Bronich, T. K.; Kabanov, V. A. *J. Am. Chem. Soc.* **1998**, *120*, 9941.

(5) Firouzi, A.; Atef, F.; Oertli, A. G.; Stucky, G. D.; Chmelka, B. F. *J. Am. Chem. Soc* **1997**, *119*, 3596.

(6) Faul, C. F. J.; Antonietti, M. *Adv. Mater.* **2003**, *15*, 673.

(7) Thalberg, K.; Lindman, B.; Karlstrom, G. *J. Phys. Chem.* **1991**, *95*, 6004.
(8) Svensson, A.; Norrman J.; Piculell, L. *J. Phys. Chem. B* **2006**, *110*, 10332.
(9) Fontell, K.; Khan, A.; Lindström, B.; Maciejewska, D.; Puang-Ngern, S. *Colloid Polym. Sci.* **1991**, *269*, 727.
(10) Oliveira, C. L. P. TRAT1D—Computer Program for SAXS Data Treatement, LNLS Technical Manual MT01/2003.
(11) Evans, D. F.; Wennerström, H. *The Colloidal Domain—where physics, chemistry, biology and technology meet*, 2nd ed.; John Wiley & Sons: New York, 1999.
(12) Rädler, J. O.; Koltover, I.; Salditt, T.; Safinya, C. R. *Science* **1997**, *275*, 810.
(13) Kekicheff, P.; Cabane, B. *J. Phys., Lett.* **1984**, *45*, L-813.
(14) Kekicheff, P.; Cabane, B.; Rawiso, M. *J. Colloid Interface Sci.***1984**, *102*, 51.
(15) Wennerström, H. *Langmuir* **1990**, *6*, 834.
(16) Slack, N. L.; Davidson, P.; Chibbaro, M. A.; Jeppesen, C.; Eiselt, P.; Warriner, H. E.; Schmidt, H. W.; Pincus, P.; Safinya, C. R. *J. Chem. Phys.* **2001**, *115*, 6252.
(17) Montalvo, G.; Khan, A. *Langmuir* **2002**, *18*, 8330.
(18) Cabane, B.; Zemb, T.; Dubois, M.; Dem, B. *Colloids Surf. A* **1997**, *121*, 135.
(19) Ruppelt, D.; Kötz, J.; Jaeger, W.; Friberg, S. E.; Mackay, R. A. *Langmuir* **1997**, *13*, 3316.
(20) Bernardes, J. S.; Loh, W., unpublished results.
(21) Kunieda, H.; Shigeta, K.; Suzuki, M. *Langmuir* **1999**, *15*, 3118.
(22) Kunieda, H.; Ozawa, K.; Huang, K.-L. *J. Phys. Chem. B* **1998**, *102*, 831.
(23) Ilekti, P.; Piculell, L.; Tournilhac, F.; Cabane, B. *J. Phys. Chem. B* **1998**, *102*, 344.
(24) Vethamuthu, M. S.; Almgren, M.; Bergenstahl, B.; Mukhtar, E. *J. Colloid Interface Sci.* **1996**, *178*, 538.
(25) Bilalov, A.; Leal, C.; Lindman, B. *J. Phys. Chem. B* **2004**, *108*, 15408.
(26) Guldbrand, L.; Jönsson, B.; Wennerström, H.; Linse, P. *J. Phys. Chem.* **1984**, *80*, 2221.
(27) Turesson, M.; Forsman, J.; Akesson, T.; Jönsson, B. *Langmuir* **2004**, *20*, 5123.
(28) Linse, P.; Lobaskin, V. *Phys. Rev. Lett.* **1999**, *83*, 4208.